

Submicron ripple formation on glass surface upon laser-nanosphere interaction

Senthil Theppakuttai and Shaochen Chen^{a)}

Department of Mechanical Engineering, The University of Texas at Austin, Texas 78712

(Received 10 December 2003; accepted 9 February 2004)

Submicron ripples have been observed on a borosilicate glass surface when irradiated by a nanosecond Nd: yttrium–aluminum–garnet laser (10 ns, 1064 nm), using silica nanospheres. The ripples thus obtained do not satisfy Rayleigh's diffraction condition in that (a) the ripple spacing is different from the value predicted by the classical model, (b) the spacing is independent of the incident angle, and (c) the orientation is not always perpendicular to the laser polarization. Also, the ripple characteristics are not dependent on the diameter of the spheres used and the ripples have almost the same periodicity irrespective of the experimental parameters. Photoionization followed by a self-organization process due to nonlinear absorption of the enhanced optical field between the spheres and glass sample is believed to be the primary reason for the creation of ripples on the glass substrate. © 2004 American Institute of Physics. [DOI: 10.1063/1.1690858]

I. INTRODUCTION

A phenomenon frequently observed during the illumination of solid surfaces with a single uniform laser beam of sufficient intensity is the appearance of spontaneous periodic surface structures or ripples. These grating like damage patterns have been produced on the surface of a variety of materials^{1,2} as well as within the bulk of dielectrics using cw to femtosecond laser sources operating over a wide range of wavelengths (0.17–10.6 μm). Very similar ripples are also observed in a large variety of experiments on laser-assisted film growth,³ laser etching,⁴ photodeposition,^{5,6} and other laser material processing.⁷ Quite frequently ripples are seen at incident laser energies just below the damage threshold for the material, indicating that high intensities are not necessary for ripple production. Due to the wide variety of experimental conditions under which these ripples have been produced, several mechanisms have been proposed to explain the observation of ripples. For example, suggestions have been put forward involving laser-acoustic-mode coupling,⁸ driven surface plasmons,⁹ or even Bose–Einstein condensation of bulk plasmons.¹⁰

Although it is possible to form ripples with single pulses, the patterns so formed can be influenced by the presence of isolated defects or scratches. The observation of fringes near a scratch indicate that at least for a wide class of materials surface roughness is responsible for the symmetry breaking necessary to produce periodic surface damage. The ripple spacing is λ for semiconductors and metals, whereas those observed on wide bandgap dielectrics are spaced at λ/n for normal incidence, where λ is the wavelength of the laser, and n is the index of refraction.¹¹ Another model which takes into account the polarization charge induced on the boundaries of defects by the applied field has also been proposed. According to this model, linearly polarized radiation incident upon linear defects aligned perpendicular to the polarization direc-

tion produced the largest perturbation, while the perturbation was zero for defects running parallel to the incident polarization direction.¹²

During laser surface melting and alloying, ripples have been observed on surfaces of metals and alloys. These ripples can result from the vapor pressure above the molten film depressing the film,¹³ surface tension of the molten film pushing the liquid film in a nonplanar meniscus shape, and the shear stresses on the molten film caused by gradients in surface tension of the liquid film.¹⁴ In case of fused silica under normal incidence of linearly polarized light from a pulsed CO₂ laser, the fundamental mechanism of ripple formation is attributed to the generation of capillary waves owing to vapor recoil pressure and nonuniform removal of substance from the surface by evaporation.¹⁵

Ripples have also been observed in photochemically deposited thin metal films. In photodeposited carbon films, the ripple generation is associated with irradiation near strong absorption bands of the parent and product compounds together with dipolar scattering.¹⁶ However, it is generally agreed that in most metallic films, the ripple formation involves scattering of the incident waves into surface waves. The spatial modulation of optical intensity resulting from the interference between the incident wave and surface-plasma waves (SPW) promotes the exponential growth of ripples, which increase the scattering into SPW thereby creating a positive feedback effect. The scattered spatial frequency component having the largest exponential gain ultimately dictates the final ripple structure upon solidification of the material.¹⁷

In nearly all of the earlier mentioned work, the crests and valleys of the ripples are mostly found to run perpendicular to the incident electric field. The ripple period can be calculated with an accuracy of a few percent from Rayleigh's diffraction criterion as given by¹

$$\Lambda = \frac{\lambda}{n_0[1 \pm \sin \theta]}, \quad (1)$$

^{a)}Electronic mail: sschen@mail.utexas.edu

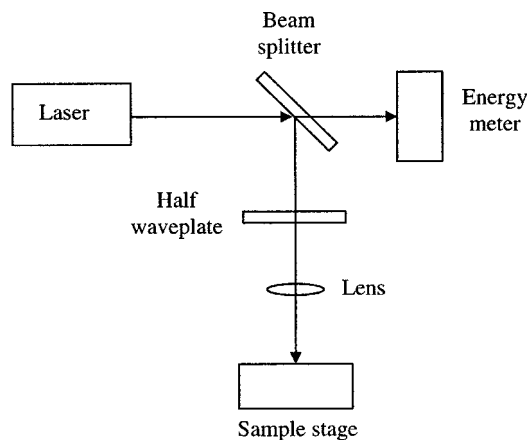


FIG. 1. Schematic of the experimental setup.

where λ is the laser wavelength, n_0 is the refractive index of the medium, and θ is the angle of incidence measured from the normal to the surface.

In this work, we observe submicron ripples when a monolayer of silica nanospheres are deposited on a glass substrate and exposed to laser irradiation from the glass side. The experiments are performed for different sphere sizes, varying angle of incidence and laser polarization. Finally, scanning electron microscopy (SEM) and atomic force microscopy (AFM) are used to characterize the ripples.

II. EXPERIMENTAL SETUP

The schematic of the experimental setup is shown in Fig. 1. A 1064 nm Nd:yttrium–aluminum–garnet laser of 12 ns pulse width is used as the illumination source in our experiment. The output laser beam, which is *s*-polarized, is split into two beams by using a beam splitter. One part of the beam is used for measuring the laser energy with the help of an energy meter and the other part is passed through a half waveplate mounted on a rotary mount. Rotating the waveplate changes the polarization of the incoming beam from *s*-polarization to *p*-polarization and vice versa. The laser beam coming out of the waveplate is then focused onto the sample, using a plano-convex lens. The sample is loaded on a three-dimensional stage capable of motion in all three directions.

The sample used in the experiment is borosilicate glass of thickness 500 μm . The wafers are well polished and, hence, the surface roughness is in nanometer scale (<2 nm). The samples are cleaned in ethanol solution followed by rinsing in de-ionized water to make sure the sample is clean and free of any contaminants. After the samples are dried with nitrogen gas, an aqueous solution of monodispersed silica nanospheres (1.76 μm and 640 nm diameter) diluted with de-ionized water is applied on the glass sample. After the evaporation of water, the nanospheres reorganize and form a hexagonally close-packed monolayer on the glass substrate by means of a self-organizing process.

After confirming the hexagonal monolayer arrangement, the glass samples are exposed to the laser beam from the backside as shown in Fig. 2. Borosilicate glass is transparent to the wavelength used in our experiment and, hence, the

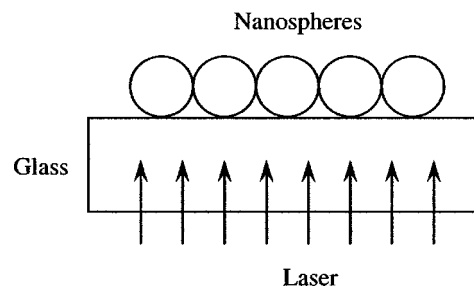


FIG. 2. Schematic of the irradiation of silica spheres on glass from the backside.

laser beam passes through the glass substrate and is incident on the bottom side of the monolayer of spheres. When the nanospheres are illuminated by the laser beam, the incident light intensity is enhanced and an optical near-field is produced around the spheres. As a result, periodic grating like structures are created on the glass surface and the ripple characteristics are studied in detail using an optical microscope, SEM, and AFM.

III. RESULTS AND DISCUSSION

A monolayer of 640 nm spheres is deposited on the glass substrate and a SEM micrograph of the monolayer is presented in Fig. 3. The glass sample is then illuminated by a single *s*-polarized laser pulse of 10 mJ/cm^2 from the glass side at an incident angle of 0° . The spheres are ejected from the glass surface and periodic surface structures are formed on the surface of the glass substrate. These structures are characterized as long, parallel lines extending over the entire laser exposed area as shown in the SEM micrograph in Fig. 4. The periodicity of the ripples (horizontal spacing between two crests or valleys) thus created is found to be 450 nm. AFM cross section of the surface shows that the ripples are indeed undulations of the surface and the profile varies sinusoidally with an amplitude variation of around 80 nm as shown in Fig. 5. To investigate the ripple characteristics in detail, the experiment is repeated by changing the angle of incidence of the laser beam onto the target. Varying the incident angle from 0° to 45° had no influence on the formation of ripples and the spacing remains the same. For both 0° and 45° incidence of the *s*-polarized laser beam, the ripples are oriented perpendicular to the electric field (E) of the in-

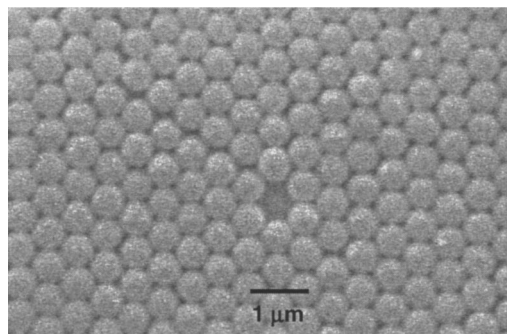


FIG. 3. SEM micrograph of a hexagonally close-packed monolayer of silica nanospheres of 640 nm in diameter on a glass substrate.

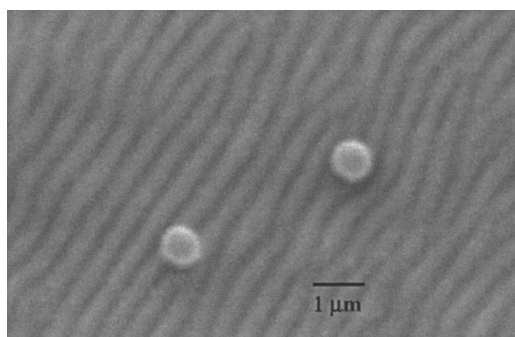


FIG. 4. SEM micrograph of the ripples extending over the entire laser exposed area for 640 nm spheres at 0° incidence of an s -polarized laser beam.

cident beam. The experiment is repeated for a p -polarized laser beam at 0° and 45° incident angles. The ripples obtained under these conditions again have the same periodicity. However, with a p -polarized incident beam, the ripples are oriented parallel to the electric field instead of the perpendicular orientation observed with an s -polarized beam.

To better understand the ripple formation mechanism, we repeated the experiments with $1.76 \mu\text{m}$ diameter spheres. It is found that the diameter of the spheres does not influence

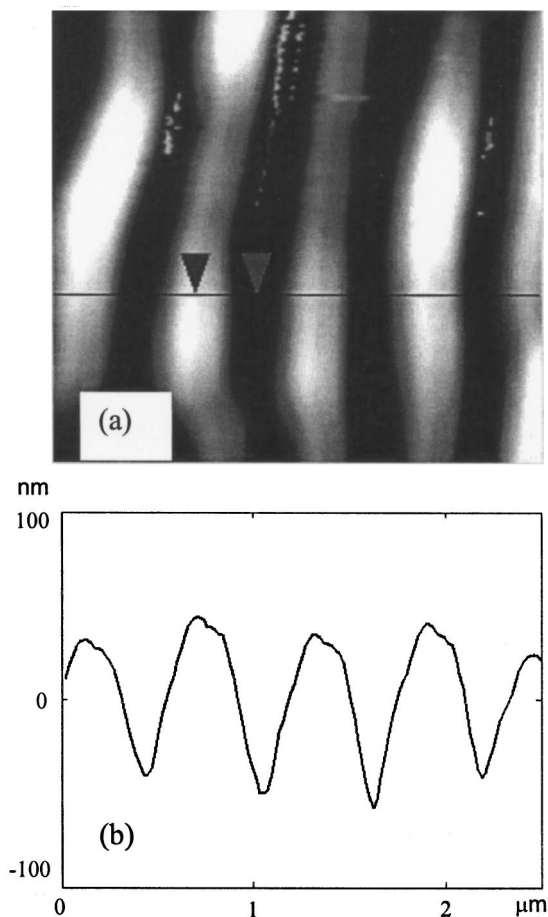


FIG. 5. AFM traces showing the cross-section profile of the ripples created with 640 nm spheres for 0° incidence of an s -polarized laser beam: (a) surface topography and (b) cross-section profile.

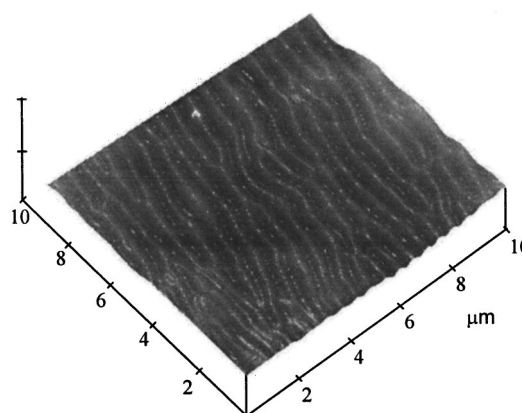


FIG. 6. AFM image of the ripples created with $1.76 \mu\text{m}$ spheres for 45° incidence of a p -polarized laser beam.

the ripple characteristics, i.e., the spacing and amplitude remain 450 and 80 nm, respectively, for both s -polarized and p -polarized laser beams at 0° as well as 45° incidence. The ripples are again oriented perpendicular to the electric field in case of an s -polarized incident beam, whereas the orientation is parallel to the electric field in case of a p -polarized beam. An AFM image of the ripples obtained with $1.76 \mu\text{m}$ spheres for 45° incidence of a p -polarized laser beam is presented in Fig. 6.

Thus, the ripple formation mechanisms proposed earlier do not provide a satisfactory explanation for the ripples observed in our experiment. Also for dielectrics, no surface excitations like surface plasmons exist in the visible or near-infrared, and for these materials a wave propagating parallel to the surface with a wavelength λ or indeed with any wavelength does not satisfy the Maxwell boundary conditions across the interface.¹⁸

In laser ablation of wide band gap transparent dielectrics using an ultrafast laser pulse, multiphoton surface ionization followed by Coulomb explosion of positive ions from an electrostatically unstable surface is believed to be the prominent mechanism for material removal.¹⁹ In patterning glass using nanospheres, the presence of an enhanced optical field around the spheres is believed to induce nonlinear absorption. The nonlinear absorption resulting from the laser-sphere interaction has been used to create submicron features on glass.²⁰ In this work, the enhanced optical field around the spheres results in an electrostatically unstable surface due to multiphoton ionization, finally leading to an explosive emission of ions. However, the whole electrostatically driven ablation mechanism comes against the idea of ripple formation, which corresponds to a phase transition. Therefore, as suggested by Reif *et al.*,^{21,22} the generation of a strongly perturbed surface in an extremely short time leads to a self-organization process during the relaxation of the surface instability. Thus, we believe self-organization mechanism to be the main cause for the formation of ripples. Though this model cannot explain the role of polarization, investigation to support this view is currently underway.

IV. CONCLUSIONS

Submicron ripples have been observed on a glass surface by depositing a monolayer of silica nanospheres and irradiating with a laser beam. The ripples thus formed are parallel and periodic extending over the entire spot. The spacing of the ripples obtained in our experiment does not satisfy the Rayleigh's diffraction criterion and they are also independent of the sphere diameter and incident angle. However, their orientation is perpendicular to the electric field while using an *s*-polarized beam and parallel to the electric field in case of a *p*-polarized beam. Self-organization during the surface instability is believed to be responsible for the formation of submicron ripples.

ACKNOWLEDGMENTS

This work was supported by research grants from the US National Science Foundation (Nos. DMI 0222014 and CTS 0243160). The SEM measurement was conducted in the Texas Materials Institute and the AFM measurement was done in the Center for Nano and Molecular Science and Technology at the University of Texas at Austin.

¹Z. Guosheng, P. M. Fauchet, and A. E. Siegman, Phys. Rev. B **26**, 5366 (1982).

- ²J. E. Sipe, J. F. Young, J. S. Preston, and H. M. van Driel, Phys. Rev. B **27**, 1141 (1983).
- ³N. R. Isenor, Appl. Phys. Lett. **32**, 535 (1978).
- ⁴N. Tsukada, S. Sugata, and Y. Mita, Appl. Phys. Lett. **43**, 189 (1983).
- ⁵S. R. J. Brueck and D. J. Ehrlich, Phys. Rev. Lett. **48**, 1678 (1982).
- ⁶R. M. Osgood, Jr. and D. J. Ehrlich, Opt. Lett. **7**, 385 (1982).
- ⁷A. K. Jain, V. N. Kulkarni, D. K. Sood, and J. S. Uppal, J. Appl. Phys. **52**, 4882 (1981).
- ⁸G. N. Maracas, G. L. Harris, C. A. Lee, and R. A. McFarlane, Appl. Phys. Lett. **33**, 453 (1978).
- ⁹J. F. Young, J. E. Sipe, and H. M. van Driel, Opt. Lett. **8**, 431 (1983).
- ¹⁰J. A. van Vechten, Solid State Commun. **39**, 1285 (1985).
- ¹¹M. J. Soileau, IEEE J. Quantum Electron. **QE-20**, 464 (1984).
- ¹²P. A. Temple and M. J. Soileau, IEEE J. Quantum Electron. **QE-17**, 2067 (1981).
- ¹³H. E. Cline and T. R. Anthony, J. Appl. Phys. **48**, 5096 (1977).
- ¹⁴T. R. Anthony and H. E. Cline, J. Appl. Phys. **48**, 3888 (1977).
- ¹⁵V. I. Emel'yanov, V. I. Konov, V. N. Tokarev, and V. N. Seminogov, J. Opt. Soc. Am. B **6**, 104 (1989).
- ¹⁶R. J. Wilson and F. A. Houle, Phys. Rev. Lett. **55**, 2184 (1985).
- ¹⁷D. J. Ehrlich and S. R. Brueck, Appl. Phys. Lett. **47**, 216 (1985).
- ¹⁸J. F. Young, J. E. Sipe, J. S. Preston, and H. M. van Driel, Appl. Phys. Lett. **41**, 261 (1982).
- ¹⁹J. T. Dickinson, J. J. Shin, and S. C. Langford, Appl. Surf. Sci. **96-98**, 316 (1996).
- ²⁰S. Theppakuttai and S. C. Chen, Appl. Phys. Lett. **83**, 758 (2003).
- ²¹F. Costache, M. Henyk, and J. Reif, Appl. Surf. Sci. **186**, 352 (2002).
- ²²J. Reif, F. Costache, M. Henyk, and S. V. Pandelov, Appl. Surf. Sci. **197-198**, 891 (2002).